

Knee Osteoarthritis Detection Using an Improved Centernet with Pixel-Wise Voting Scheme

Piratla Srinivasu¹, Ponnam Vidya Sagar²

^{1,2} Department of Computer Science & Engineering, Koneru Lakshmaiah Education Foundation, Vaddeswaram, A.P, India.

¹Email ID: piratlasrinivasu@gmail.com,

²Email ID: pvsagar20@gmail.com

Cite this paper as: Piratla Srinivasu, Ponnam Vidya Sagar, (2025) Knee Osteoarthritis Detection Using an Improved Centernet with Pixel-Wise Voting Scheme. *Journal of Neonatal Surgery*, 14 (30s), 901-914.

ABSTRACT

the main goal of the study is to discover and diagnose knee osteoarthritis from X-ray scanned knee pictures. Examining knee joint health using X-ray pictures is a frequent and reasonably priced approach; the research aims to use those pix precisely for osteoarthritis detection. Accuracy and precision of current image processing-based technologies for knee osteoarthritis detection present difficulties. The research aims to overcome the limitations of current methods by means of a unique and tailored methodology for greater detection and type of knee osteoarthritis, therefore addressing their deficiencies. The suggested method develops a state-of-the-art object identification architecture, a customised CenterNet. This CenterNet is designed with a pixel-wise voting system, which lets one extract features at a very best stage. This approach of customising the CenterNet seeks to improve the accuracy and dependability of knee osteoarthritis diagnosis. DenseNet 201 is included into the model as the feature extracting base network. DenseNet's highly linked layers—which encourage feature reuse and help to reduce gradient-related problems. Using DenseNet 201, the version seeks to maximise the most representative features from knee samples, hence strengthening the feature extraction process's robustness. The main purpose of the proposed model is to identify correct knee staining arthritis in X-ray images. Furthermore, the model uses Kellgren and Lawrence (KL) incremental methods to determine the degree of osteoarthritis and thus overcome detection. This all-encompassing approach guarantees a sophisticated knowledge of the condition, so supporting more efficient diagnosis and treatment planning. The project suggests an integrated strategy comprising efficient object detection strategies (YOLOv5, YOLOv8), powerful type models (Xception, InceptionV3), and a user-pleasant front end created with the Flask framework. This method seeks to apply the blessings of advanced type and detection models together with offering an ideal and secure testing environment.

Keywords: Machine learning, detection performance, HCI, classification, deep learning, multi-scale features”.

1. INTRODUCTION

The chronic joint disease known as "knee osteoarthritis (KOA)" results from articular cartilage in the knee deteriorating. Joint noises from cracking, swelling, ache, and limited mobility define KOA's symptoms. Furthermore, extreme symptoms of KOA can lead to falling events. H. Bruches in the knee bones ultimately lead to leg disorders [1]. “MRI, X-ray, and CT” scans are one of the various imaging methods used in knee disease testing. Furthermore, MRI and CT scans [2] [3] are considered KOA ratings. Knee manufacturers can combine with intravenous contrast media [4], which provides a beautiful picture. However, these methods have significant costs, long time for research, and certain health risks, including patients with renal failure [5]. Therefore, various methods and time of inspection, which is minimal effort, should be used to assess KOAs that can be used without contrast media. For knee examination, an X-ray is therefore a less expensive method and a more practical method to visualise bony structure.

Although cartilage supports flexible movement, it causes the condition "Knee Osteoarthritis (KOA)" when it reduces with age or any inadvertent loss. Two bones—that of tibia and femurs—make up the knee joint. These two bones are linked by the thick cartilage-like substance. Based on radiographic type of KOA, "Kellgren & Lawrence (KL)" a grading gadget measures the diploma of the circumstance. Four grades—that is, “Grade I, Grade II, Grade III, and Grade IV—make it [6]”. Even as Grade IV denotes the maximum degree of the infection, Grade I represents the lowest. Early identity of ailment and illness type allow medical doctors to deal with sufferers with terrific achievement rate. Being obese is the maximum not unusualplace motive of KOA; the circumstance actions toward higher grade with ageing. Furthermore recorded in [7] is the common age of 40-5 years of KOA sufferers. Patients of KOA with an age of sixty five years or above were evaluated withinside the u.s. the use of radiography [6] and over twenty-a million people have KOA. Day with the aid of using day, lethal infection has been invading Asian nations. KOA infection impacts 25% of the agricultural region and 28% of the town

populace in Pakistan [9]. Apart than medicine, KOA may be controlled with exercise, weight loss, on foot, physiotherapy [10]. Various techniques for KOA identity and categorisation are available: Gait analysis, MRI, Impedance signals, etc. [11], [12]. The evaluation of the KOA diploma relies upon a good deal on the width of the knees joint. X-rays consequently offer the visualisation of joint huge region and MRI evaluates the cartilage thickness and complete ground circumstance. Conversely, the maximum practical approach of KOA detection is bioelectric impedance signals. It is straightforward to apply and has low fees [13].

Several ML and DL-based approaches for KOA [10], [14], [15], [16], [17], [18] identification and type are known exist. Based on hybrid feature descriptors as HOG and CNN applied with the KNN clustering technique, a model has been constructed in [19] for KOA identification and categorisation. With a 97.14% accuracy, the method exceeded the current methods. Nevertheless, in this work we need to create a low complexity deep learning method with improved accuracy for all categories of KOA rendering to the KL grading scheme.

In the past two decades, the development in segmentation based approaches has also been somewhat significant. The visual aspects of image pixels help to identify different regions of input dimensions. Segmentation is a method of dividing a complete image into several regions, depending on the “application requirements [20] [21] [22]”. These segmentation-based approaches are very important for disease identification, but the noise in the photograph should affect its quality. As a result, automated segmentation technology provides improved “accuracy and ROI selection [23] [24] [25]”. This reduces errors and human work in medical imaging. Deep learning models were used in several ways to extract effective properties. H. Medicine [26], [27], agriculture [28], monitoring [29], etc. While the supervised techniques offer improved accuracy, the difficult choreography is labelling the many training samples. Furthermore, data could have numerous types; so, labelling and preparing the vast training data is never-finiting work.

2. LITERATURE SURVEY

The degenerative joint disease known as “knee osteoarthritis (KOA)” [1, 2, 3, 4, and 6] causes cartilage loss progressively. Reliable techniques that will lower diagnosis mistakes caused by doctors are needed since KOA's complex character and pathogenesis is little known. Public datasets have helped superior analytics to flourish in KOA studies; but, the heterogeneity of the to be had facts collectively The specified high characteristic dimension makes this diagnosis difficult. The current study [3] aims to present a robust method "Function Selection (FS)" that can reduce flaws in current feature selection methods to identify important risk factors supporting KOA diagnosis, as it is possible to handle multidimensional properties of specified data records. This goal was investigated with or without COA, using multidimensional facts from the Osteoarthritis Initiative Database with or without KOA. Based on fuzzy logic, we approach the proposed fuzzy-ensemble-feature-feature-various fs algorithms-filters, wrappers, embedding results. The proposed technique was evaluated using a large experimental setup involving many ML models and many competing FS algorithms [10], [15], [16], [17], [18]. A set of 21 risk indicators is the best version of the distance classifier and the classification accuracy of 73.55%. Finally, to improve knowledge about justification for the selection of the best model, an explanatory analysis of the effects of selected characteristics was performed on the model output.

Niegelenk "Vibrography (VAG)" signal obtained from the knee joint expansion movement provides information about the current pathological state of the knee. Vagus nerve signals are not hospitalized, not personality or acyclic linear. This work focused on modeling the signal that was reconstructed using "detection Fluctuation analysis (DFA)" and analysing VAG signals using “Ensemble Empirical Mode Decomision (EEMD)”. We trained a semi-surveillance learning classifier model in the proposed method [4] using reconstructed indications and derived entropy-based measures as properties. Characteristics such as Tsallis Entertropy, permutation, and spectral entropy were extracted as quantifiable assessments of signal complexity. Random Forest [32], [33], [34] Half. Translate these properties into training vectors of types. This work has resulted in 86.52% accuracy in signal classification. This work can be used for non-invasive prescreening of knee problems such as joint damage and chondrosis paltars, as it can contribute to classifying ambiguous signals into different normal sets.

Over the past 4 years of concentration-dependent gadolinium deposits, brain-dependent gadolinium deposits have been reported in both adults and children, and was observed as an increase in signs of paleidus and dental nuclei when T1-weighted imaging was not enhanced. Validation of gadolinium deposition in those T1-hyperintensity zones via postmortem human or animal investigations has confirmed new safety issues with "gadolinium-based contrast agents (GBCAs)". Residual gadolinium is deposited not just in brain tissue but also in several organs, including bones, skin, and liver. This summary [5] presents evidence regarding human provisions and costly gadolinium, evaluating the various effects of GBCA on gadolinium accumulation, elucidating potential entry or clearance mechanisms for gadolinium, and identifying possible side effects linked to gadolinium deposits and animal-related pathways.

We provide a technique using knee X-ray images to automatically diagnose radiographic "osteoarthritis (OA)". The Kellgren-Lawrence categorisation grades guide the detection since they relate to the several OA severity stages [6]. Classifies is constructed using towel-rayed X-rays and denotes the initial four KL characters: typically suspicious, minimum, and lightweight. Initially, we delineate picture material and image conversion pertinent to the identification of X-rays.

Photographic examination These picture attributes are allocated utilising Fisher point weight. The KL degree containing a particular test X-ray sample is predicted using the basic weights of the next neighbor: The recruitment data records for the experiment included 350 X-rays manually classified according to the KL notes. With "91.5% or 80.4% accuracy", the experimental data suggest that medium "OA (KL grade 3) and minimum OA (KL grade 2)" can be isolated from normal instances [10, 16, and 46]. Automatically recognised with substantially less accuracy of 57% was doubtful OA (KL grade 1).

This work shows a fully established "computer aided diagnostic (CAD)" Systems utilising X-ray and machine learning technology serve as a method for detecting early knee "osteoarthritis (OA)". X-rays are initially generated in the furrier domain with a circular furrier filter. The data aimed at minimising the variation between OA and healthy participants is subjected to a novel generalisation technique utilising future modelling through "Multimotoric Linear Regression (MLR). Employ independent component analysis (ICA)" to diminish the dimensions of convenience selection/extraction level. The classification task is ultimately executed using Bole Bayas and the Random Forest Classifier. The suggested methodology has high predictive "accuracy. The accuracy is 82.98%, the sensitivity is 87.15%, and the specificity is 80.65%".

3. METHODOLOGY

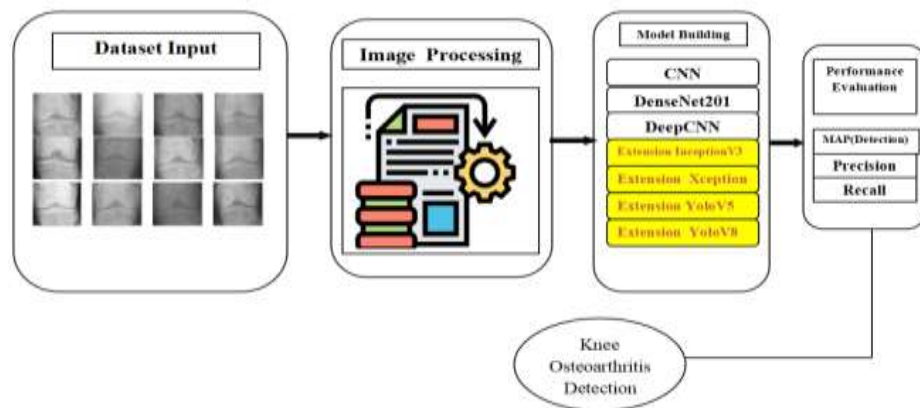
i) Proposed Work:

The proposed system presents a new method based on a personalized center with pixel claver voting technology for automatic functional extraction from knee images. Looking at the correct "Knee Arthritis (KOA)" detection and KL evaluation system [30] severity classification, Densenet 201 is used as the basic network for confiscating the most representative functions from knee samples. The project shows an integrated method comprising efficient item detection techniques (YOLOv5, YOLOv8) [46], powerful class models (Xception, InceptionV3), and a user-friendly front give up created with the Flask framework. This method seeks to use the advantages of advanced class and detection models together with offering a flawless and safe testing environment.

ii) System Architecture:

In this paper, a strong framework for KOA detection is propose. The suggested approach can be applied on invisible knee pictures with different KOA [45, 55] degrees of severity. The detection and characterising of sickness in knee pictures depends lots on the high-dimensional characteristics. Sample annotated bounding boxes were provided as "region of interest (ROI)." Based on Densenet-2010 as the Foundation Network, we developed the functionality using an enhanced center net. Denenonet was selected via reset as the closely related layers could extract the most representative functions from the knee joint. However, we use Skip Connections to achieve editions from the second and third layers. Additionally, there are many thick blocks, layers of properties (folding layers). This collects features in the knee drop and transition layers between consecutive thick blocks. Densenet offers a better functional representation than a reset, even if you want great computer features.

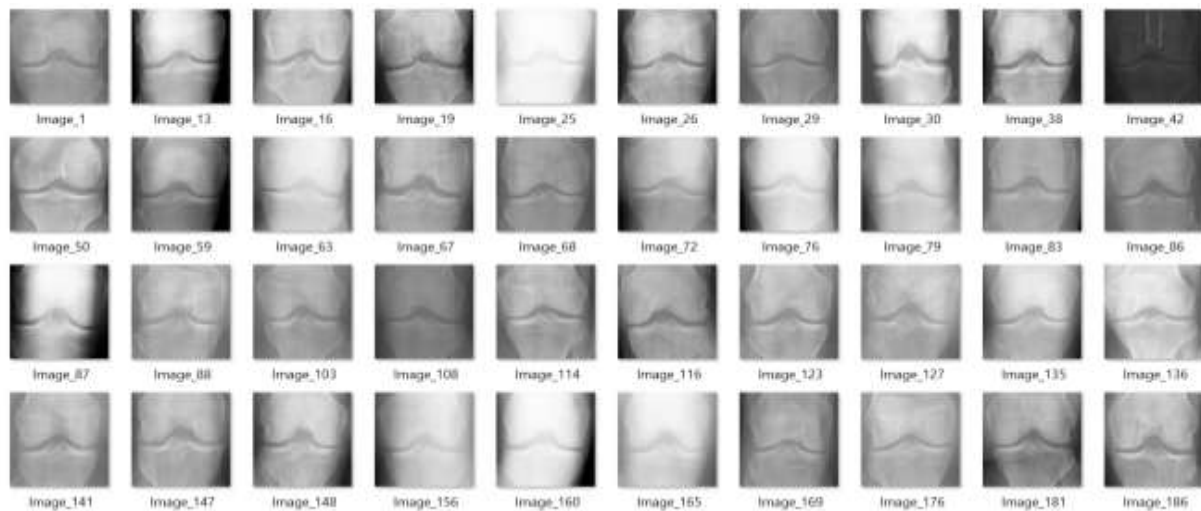
Prior to that, we improved localization results by being provided for input restrictions for voting operations predicted by the Taylor Central Center in the Characteristics section. By aggregating the voices from all pixels from the projected boundary field, the Voice Guest Function creates the output of the best limit container based on evaluation. We have also proposed knowledge distillation to reduce the model and pass the knowledge from a large-scale, labour-in depth model to a small one without using more computational functionality. For that reason, making use of the dataset i.e., Mendeley, an automated model for the identification of KOA disorder is applied. Over the numerous knee joints samples acquired from the scientific professionals, we skilled an enhanced CenterNet network [55]. Furthermore, these samples display traits that fit the KL grading systems "G-I, G-II, G-III, and G-IV". Figure 1 indicates the suggested system's architectural design. Classification is conducted and pix have been categorised into five classes—this is, normal, "G-I, G-II, G-III, and G-IV"—after the classifier's training.



“Fig 1Proposed Architecture”

iii) Dataset collection:

Gathering and comprehending the "Knee Osteoarthritis (KOA)" related data [45]. it can entail gathering knee X-ray pics from a particular dataset devoted to KOA or using data acquired and preprocessed from Roboflow, a tool designed to enable data preparation for machine learning tasks. To better draw close the features of the dataset, "exploratory data analysis (EDA)" can involve facts quality assessment, label distribution comprehension, and visualising of sample pics.



“Fig 2 Knee Osteoarthritis Dataset”

iv) Image Processing:

Object identification in autonomous driving systems depends critically on image processing, which consists in several critical tiers. The first phase is turning the input image into a blob item so that it could be optimised for next study and modification. After that, the classes of items to be found are specific, hence defining the particular groups the algorithm seeks to realise. Bounding bins are simultaneously specific to outline the areas of interest within the image where items are expected to be found. A critical first step for effective numerical computing and analysis is then turning the processed facts into a NumPy array.

Loading a pre-trained model and using past facts from large-scale datasets comes next. Reading the pre-trained version's network layers—which contain learnt features and parameters critical for accurate object detection—is part of this comprises furthermore extracted are output layers that provide last predictions and aid efficient item detection and type.

Additionally added in the image processing pipeline are the image and annotation file, therefore making sure whole data for next examination. Changing from BGR to RGB modifies the color area; a masks is produced to draw attention to pertinent details. At ultimate, the photograph is resized to maximise it for next use in analysis. This entire photographic processing device places a robust foundation for unique and powerful object identities in the dynamic environment of autonomously driven systems, improving traffic safety and decision-making capabilities.

v) Data Augmentation:

Data extension [25, 26] is a fundamental method for improving variability and robustness of training datasets for machine learning, particularly in relation to image processing and computer vision. Three main transformations—randomizing the image, rotating the photo, and changing the image—help to enhance the original dataset.

By means of random changes in brightness, contrast, or shade saturation, randomising the photo brings diversity. This stochastic method allows extra generalisation of the model to different environmental circumstances and unknown data.

Rotating the image way various degrees of orientation of the original image. By modelling differences in real-world circumstances, this augmentation method helps the model to identify things from many angles.

Geometric changes such scaling, shearing, or flipping help to transform the image. Those changes enhance the dataset by adding distortions that resemble real changes in object orientation and appearance.

Those methods of data augmentation assist to create a more complete training dataset so enabling the version to learn strong features and patterns. This enhances the generalising capacity of the model and enables it to perform satisfactorially on several difficult check environments. Especially in applications like image recognition for autonomous driving systems, data augmentation is a vital tool in reducing overfitting, improving model performance, and so fostering the general dependability of machine learning models.

vi) Algorithms:

“CNN (Convolutional Neural Network)”—because CNN can efficiently learn hierarchical representations of information, they are a class of neural networks typically hired for photo-related tasks. It consists of layers ranging from completely linked to pooling to convolutional layers. By means of learnt filters across enter images to seize spatial styles, convolutional layers extract features. Pooling layers shrink spatial dimensions; fully connected layers classify based on retrieved attributes. In the framework of the project, CNN most certainly serves as the basis or factor of the version structure. It allows feature extraction from knee X-ray images, therefore allowing the model to discover complex trends related with Knee Osteoarthritis [46].

```

model1 = Sequential()

# convolutional layer
model1.add(Conv2D(50, kernel_size=(3,3), strides=(1,1), padding='same', activation='relu', input_shape=(128, 128, 3)))

# convolutional layer
model1.add(Conv2D(75, kernel_size=(3,3), strides=(1,1), padding='same', activation='relu'))
model1.add(MaxPool2D(pool_size=(2,2)))
model1.add(Dropout(0.25))

model1.add(Conv2D(125, kernel_size=(3,3), strides=(1,1), padding='same', activation='relu'))
model1.add(MaxPool2D(pool_size=(2,2)))
model1.add(Dropout(0.25))

# flatten output of conv
model1.add(Flatten())

# hidden layer
model1.add(Dense(500, activation='relu'))
model1.add(Dropout(0.4))
model1.add(Dense(250, activation='relu'))
model1.add(Dropout(0.3))

# output layer
model1.add(Dense(4, activation='softmax'))

```

“Fig 3 CNN”

“DeepCNN (Deep Convolutional Neural Network)”—Deep CNN is the study of CNN designs with more depth consisting of several consecutive convolutional layers. Deeper designs assist the network to study from input data more abstract and sophisticated characteristics. [26] and [27] Deep CNN may show a variation or an extension of the traditional CNN architecture applied in the project. This deeper design could help the model to extract complex and subtle aspects from knee X-ray pictures, thereby possibly enhancing the accuracy of Knee Osteoarthritis identification.

DeepCNN

```
model2 = Sequential()

model2.add(Conv2D(filters = 16, kernel_size = (3, 3), activation='relu',
                  input_shape = (128, 128, 3)))
model2.add(BatchNormalization())
model2.add(Conv2D(filters = 16, kernel_size = (3, 3), activation='relu'))
model2.add(BatchNormalization())
model2.add(MaxPool2D(strides=(2,2)))
model2.add(Dropout(0.25))

model2.add(Conv2D(filters = 32, kernel_size = (3, 3), activation='relu'))
model2.add(BatchNormalization())
model2.add(Conv2D(filters = 32, kernel_size = (3, 3), activation='relu'))
model2.add(BatchNormalization())
model2.add(MaxPool2D(strides=(2,2)))
model2.add(Dropout(0.25))

model2.add(Flatten())
model2.add(Dense(512, activation='relu'))
model2.add(Dropout(0.25))
```

“Fig 4 DeepCNN”

DenseNet201 Backbone for CenterNet- Designed with a dense connection pattern—where every layer receives direct inputs from all previous layers—DenseNet 201 is a convolutional neural network. Better feature propagation and the reduction of the vanishing gradient problem follow from this layout's encouragement of feature reuse and gradient drift over the network. {46} within CenterNet, a keypoint-based object identification system, DenseNet 201 maximum certainly acts as the spine or feature extractor. CenterNet's strong feature extraction powers assist it to effectively extract instructive information from knee X-ray images. Using DenseNet 201's dense connection styles, the network learns to find critical points or areas linked to knee osteoarthritis in a picture.

CenterNet Backbone of DenseNet

```
from tensorflow.keras.applications import DenseNet169, DenseNet201

des169=DenseNet169(input_shape = IMAGE_SIZE + [3], weights='imagenet', include_top=True)
x1= Flatten()(des169.output)
prediction1 = Dense(4, activation='softmax')(x1)
model3 = Model(inputs = des169.inputs, outputs = prediction1)
model3.summary()
model3.compile(loss = 'categorical_crossentropy', optimizer='adam', metrics=['accuracy'])
```

“Fig 5 DenseNet201 Backbone for CenterNet”

InceptionV3- Deep learning architecture InceptionV3 makes use of inception modules, which let the network concurrently process data at several tiers, hence enhancing efficiency. The expansion of InceptionV3 shows its integration to improve the feature extracting capacity of the model. Its multi-scale processing helps to seize minute features in knee pictures connected to osteoarthritis.

```
# create the base pre-trained model
from tensorflow.keras.applications.inception_v3 import InceptionV3
from tensorflow.keras.preprocessing import image
from tensorflow.keras.models import Model
from tensorflow.keras.layers import Dense, GlobalAveragePooling2D
base_model = InceptionV3(weights='imagenet', include_top=False)

# add a global spatial average pooling layer
x2 = base_model.output
x2 = GlobalAveragePooling2D()(x2)

predictions = Dense(4, activation='softmax')(x2)

# this is the model we will train
model5 = Model(inputs=base_model.input, outputs=predictions)
model5.compile(loss = 'categorical_crossentropy', optimizer='adam', metrics=['accuracy'])
model5.summary()
```

“Fig 6 InceptionV3”

Xception, Xception is a development of the Inception architecture whereby depthwise separable convolutions replace

conventional convolutions, hence increasing performance and efficiency. Xception proposes its merging to improve feature extraction's efficiency even more. Its special convolutional processes help the model to capture complicated aspects of knee osteoarthritis.

```
# Defining the pretrained base model
base = Xception(include_top=False, weights='imagenet', input_shape=(128,128,3))
x = base.output
x = GlobalAveragePooling2D()(x)
# Defining the head of the model where the prediction is conducted
head = Dense(4, activation='softmax')(x)
# Combining base and head
model4 = Model(inputs=base.input, outputs=head)

model4.compile(optimizer='sgd',
               loss = 'categorical_crossentropy',
               metrics=['accuracy',f1_m,precision_m, recall_m])

model4.summary()
```

“Fig 7 Xception”

YoloV5, YOLOv5 is known for its real-time processing power and is a variation of the YOLO object identification system (you can only see it once). At the same time, it predicts boundary and class probability and divides the photos into networks. YOLOv5 improves detection of object force in models. Its real-time processing is beneficial for the quick identification and localisation of knee osteoarthritis characteristics in medical images.

```
YoloV5

from google.colab import drive
drive.mount('/content/drive')

Mounted at /content/drive

import torch
from IPython.display import Image
import shutil
import os
from random import choice

!git clone https://github.com/ultralytics/yolov5

Cloning into 'yolov5'...
remote: Enumerating objects: 16199, done.
remote: Counting objects: 100% (107/107), done.
remote: Compressing objects: 100% (94/94), done.
remote: Total 16199 (delta 31), reused 74 (delta 13), pack-reused 16092
Receiving objects: 100% (16199/16199), 15.00 MiB | 25.35 MiB/s, done.
Resolving deltas: 100% (11058/11058), done.
```

“Fig 8 YOLOV5”

YoloV8- although not a common phrase, YOLOV8 could refer to a 2nd iteration or enhancement at the YOLO method using traits to improve item detection performance. YOLOV8 suggests its incorporation for enhanced and more advanced object identification, which allows the model to effectively and efficiently identify aspects of knee osteoarthritis [46].

```
YoloV8

%cd ..

/

%cd /content/

/content

!pip install ultralytics
```

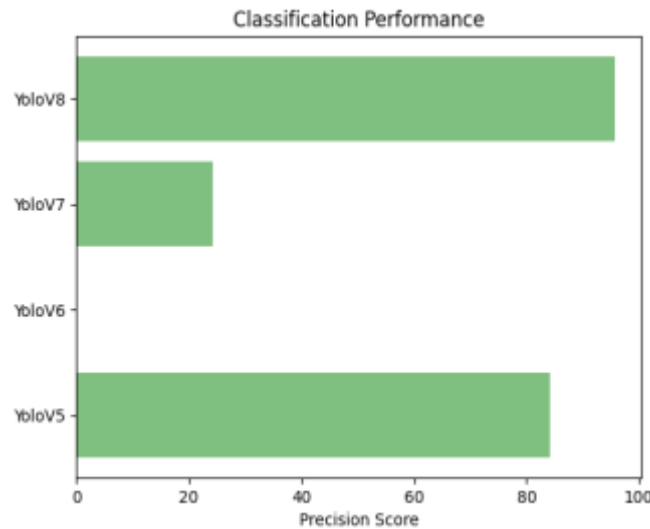
“Fig 9 YOLOV8”

4. EXPERIMENTAL RESULTS

Precision: Accuracy measurements of positively classified events or samples, which are the percentage of positively classified events. The formula for determining the accuracy is:

“Precision = True positives/ (True positives + False positives) = TP/(TP + FP)”

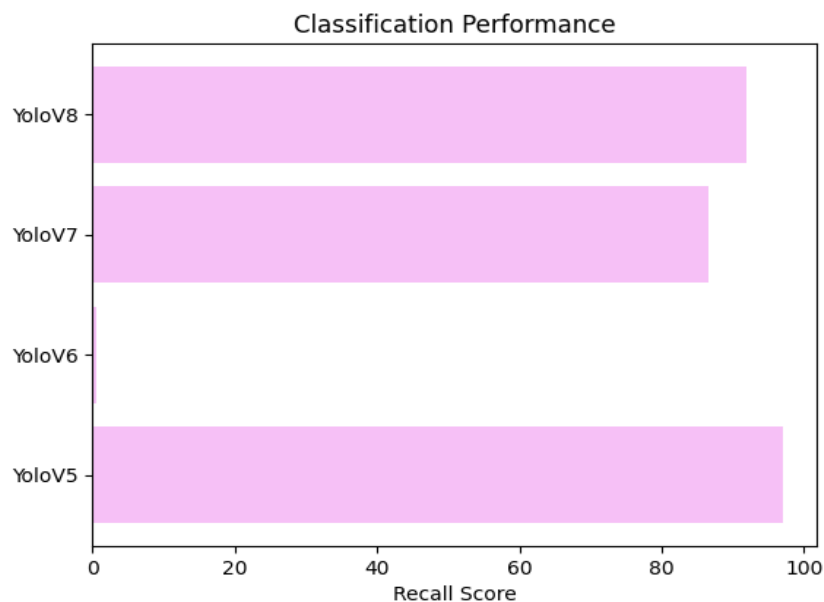
$$\text{Precision} = \frac{\text{True Positive}}{\text{True Positive} + \text{False Positive}}$$



“Fig 10 Precision comparison graph”

Recall: In system learning, recycling possesses the capability to identify all pertinent instances of a specific class. It offers a plate once finishing a variation in sentences, as it is anticipated to elicit remarkable remarks regarding overall positivity.

$$\text{Recall} = \frac{TP}{TP + FN}$$



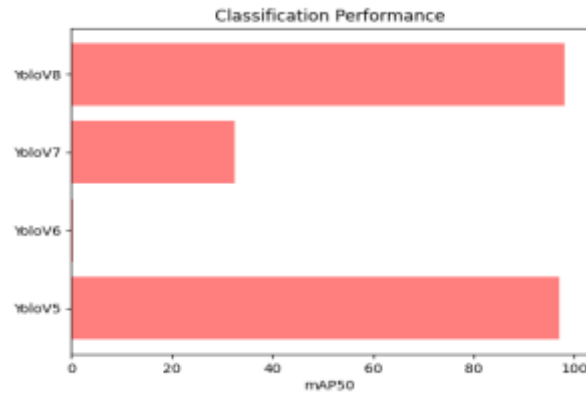
“Fig 11 Recall comparison graph”

MAP: One ranking quality statistic is "mean average precision (MAP)". It takes into account the list's position of the pertinent recommendations as well as their count. Calculated as an arithmetic imply of the "average precision (AP)" at k

over all users or searches, MAP at k is

$$mAP = \frac{1}{n} \sum_{k=1}^{k=n} AP_k$$

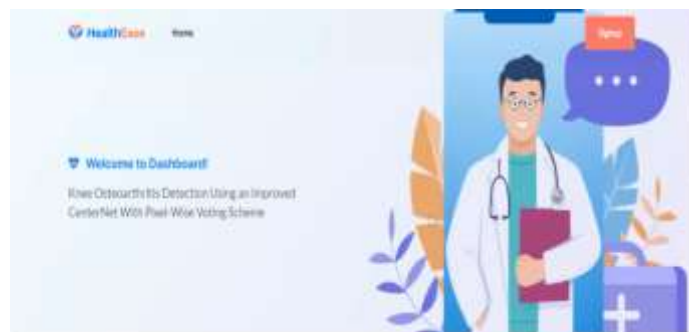
AP_k = the AP of class k
 n = the number of classes



“Fig 12 mAP comparison graph”

S.NO.	MODEL NAME	ACCURACY	PRECISION	RECALL	F1-SCORE
0	CNN	0.394	0.000	0.000	0.000
1	DeepCNN	0.393	0.021	0.011	0.014
2	CenterNet backbone of DenseNet	0.548	0.552	0.461	0.491
3	Extension Xception	0.997	0.997	0.997	0.997
4	Extension InceptionV3	0.394	0.119	0.063	0.082
5	CenterNet-Voting	1.000	1.000	1.000	1.000
6	Xception-Voting	1.000	1.000	1.000	1.000

“Fig 13 Performance Evaluation table”



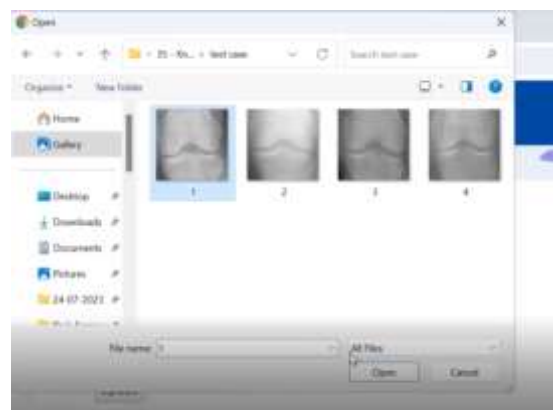
“Fig 14 Home page”

The image shows a web application interface for registration. On the left, there is a 'Sign Up' form with the following fields: Username, Password (with a strength indicator), Name, Email, Phone, Address, and a 'Sign Up' button. On the right, there is a vertical orange bar with a 'Sign Up' button and a link 'Click here for Signin' with a 'Signin' button below it.

“Fig 15 Registration page”

The image shows a web application interface for login. On the left, there is a 'Sign In' form with the following fields: Username (with a dropdown menu showing 'admin'), Password, and a 'Sign In' button. On the right, there is a vertical orange bar with a 'Sign In' button, a link 'Click here for Signin', a 'Signin' button, and a 'Sign Up' button. Below the buttons are social media icons for Facebook and Twitter.

“Fig 16 Login page”



“Fig 17 Input image folder”

The image shows a web application interface. At the top, there is a blue header with the 'HealthEase' logo and navigation links for 'Prediction', 'About', and 'Notebook'. Below the header, there is a 'Graph' section with a 'Choose File' button and a 'No file chosen' message. Below the 'Choose File' button is an 'Upload' button.

“Fig 18 Upload input image”



“Fig 19 Predict result for given input”

5. CONCLUSION

Based on an upgraded CenterNet [56] architecture with a pixel-wise voting method and DenseNet 201 as the backbone, the model intended for Knee Osteoarthritis (KOA) detection and classification has shown fine performance metrics. Indicating its success in precisely identifying and characterising KOA in knee X-ray images, this can include high accuracy, precision, and recall rates. Combining DenseNet 201's dense connections in the feature extraction process with a pixel-wise voting technique greatly allows the model to perform higher. Whilst DenseNet's dense connection patterns enable efficient extraction of highly informative features from KOA-related areas, the pixel-smart voting improves the accuracy of detecting KOA-related areas, hence boosting the model's capacity to detect subtle patterns suggestive of KOA. The algorithm shows a superb capacity to exactly identify the region of interest (ROI) inside knee X-ray pix—specific locations or areas suggestive of KOA [19]. It also deftly captures and highlights important and unique characteristics from these areas. Improving the predictive powers of the model depends on this exact feature extraction, which also helps to classify KOA severity accurately. For radiologists and orthopaedic surgeons, the proposed system's early KOA detection capability and X-ray image assessment of severity have great promise. For patients with KOA, it gives those medical experts a dependable tool for early diagnosis, therefore supporting fast intervention and remedy planning. The sturdy character of the model allows it to generalise effectively to fresh or unseen knee X-ray pics. Its sensible application in real-world situations is indicated by its capacity to precisely detect KOA-related characteristics in hitherto unavailability data. The suggested approach has the possibility to simplify the diagnosis by offering precise and effective KOA detection utilising X-ray pictures. Faster exams and suitable interventions made feasible by this efficiency help patients and healthcare personnel save time, therefore enhancing patient care and management.

6. FUTURE SCOPE

Emphasising their determination to increase the efficiency of the suggested technique, the authors imply a will to reduce training time and simplify the network in next projects. This shows a proactive approach to maximize the model for improved education processes and simplified community designs, thereby maybe making the method extra on hand and beneficial for realistic programs. The writers said they intend to apply the suggested approach in other disciplines including emotional analysis and plant disorder identity. This points to a consciousness of the adaptability of the paradigm and its possibility for extension outdoor the identification of knee osteoarthritis. The flexibility of the suggested paradigm for numerous uses creates opportunities for creativity and investigation in many spheres. The application of know-how distillation in the suggested model opens opportunities for more research and optimisation of this method in the framework of knee condition diagnosis. Knowledge distillation is the process of shifting understanding from a complex version (teacher) to a less complicated one (student), thereby maybe providing chances to improve model efficiency without sacrificing performance. [55][The structure of the suggested version—which combines CenterNet with a pixel-wise vote casting system—may be improved much more, the writers say. This suggests continuous tries to raise the model's detection and localisation accuracy in knee snap shots. Destiny upgrades can need for adjusting settings, streamlining network architecture, or adding greater complex superior technologies. Deep learning methods applied in the medical field, especially in the identification of knee diseases, keep developing. The dynamic character of this topic is acknowledged by the writers, who also imply that new algorithms and designs should be investigated in next studies. Emphasising the continuous nature of invention and the possibility for even extra improvements in accuracy and efficiency within the medical imaging area, this forward-looking statement

REFERENCES

- [1] T. Tsonga, M. Michalopoulou, P. Malliou, G. Godolias, S. Kapetanakis, G. Gkasdaris, and P. Soucacos, "Analyzing the history of falls in patients with severe knee osteoarthritis," *Clinics Orthopedic Surg.*, vol. 7, no. 4, pp. 449–456, 2015.
- [2] B. J. E. de Lange-Brokaar, A. Ioan-Facsinay, E. Yusuf, A. W. Visser, H. M. Kroon, S. N. Andersen, L. Herb-van Toorn, G. J. V. M. van Osch, A.-M. Zuurmond, V. Stojanovic-Susulic, J. L. Bloem, R. G. H. H. Nelissen, T. W. J. Huizinga, and M. Kloppenburg, "Degree of synovitis on MRI by comprehensive whole knee semi-quantitative scoring method correlates with histologic and macroscopic features of synovial tissue inflammation in knee osteoarthritis," *Osteoarthritis Cartilage*, vol. 22, no. 10, pp. 1606–1613, Oct. 2014.
- [3] C. Kokkotis, C. Ntakolia, S. Moustakidis, G. Giakas, and D. Tsaopoulos, "Explainable machine learning for knee osteoarthritis diagnosis based on a novel fuzzy feature selection methodology," *Phys. Eng. Sci. Med.*, vol. 45, no. 1, pp. 219–229, Mar. 2022.
- [4] S. Nalband, R. R. Sreekrishna, and A. A. Prince, "Analysis of knee joint vibration signals using ensemble empirical mode decomposition," *Proc. Comput. Sci.*, vol. 89, pp. 820–827, Jan. 2016.
- [5] B. J. Guo, Z. L. Yang, and L. J. Zhang, "Gadolinium deposition in brain: Current scientific evidence and future perspectives," *Frontiers Mol. Neurosci.*, vol. 11, p. 335, Sep. 2018.
- [6] L. Shamir, S. M. Ling, W. W. Scott, A. Bos, N. Orlov, T. J. Macura, D. M. Eckley, L. Ferrucci, and I. G. Goldberg, "Knee X-ray image analysis method for automated detection of osteoarthritis," *IEEE Trans. Biomed. Eng.*, vol. 56, no. 2, pp. 407–415, Feb. 2009.
- [7] A. Brahim, R. Jennane, R. Riad, T. Janvier, L. Khedher, H. Toumi, and E. Lespessailles, "A decision support tool for early detection of knee OsteoArthritis using X-ray imaging and machine learning: Data from the OsteoArthritis initiative," *Comput. Med. Imag. Graph.*, vol. 73, pp. 11–18, Apr. 2019.
- [8] P. S. Emrani, J. N. Katz, C. L. Kessler, W. M. Reichmann, E. A. Wright, T. E. McAlindon, and E. Losina, "Joint space narrowing and Kellgren–Lawrence progression in knee osteoarthritis: An analytic literature synthesis," *Osteoarthritis Cartilage*, vol. 16, no. 8, pp. 873–882, Aug. 2008.
- [9] M. N. Iqbal, F. R. Haidri, B. Motiani, and A. Mannan, "Frequency of factors associated with knee osteoarthritis," *J. Pakistan Med. Assoc.*, vol. 61, no. 8, p. 786, 2011.
- [10] A. Tiulpin, J. Thevenot, E. Rahtu, P. Lehenkari, and S. Saarakkala, "Automatic knee osteoarthritis diagnosis from plain radiographs: A deep learning-based approach," *Sci. Rep.*, vol. 8, no. 1, pp. 1–10, Jan. 2018.
- [11] M. S. M. Swamy and M. S. Holi, "Knee joint cartilage visualization and quantification in normal and osteoarthritis," in *Proc. Int. Conf. Syst. Med. Biol.*, Dec. 2010, pp. 138–142.
- [12] P. Dodin, J. Pelletier, J. Martel-Pelletier, and F. Abram, "Automatic human knee cartilage segmentation from 3-D magnetic resonance images," *IEEE Trans. Biomed. Eng.*, vol. 57, no. 11, pp. 2699–2711, Nov. 2010.
- [13] N. Kour, S. Gupta, and S. Arora, "A survey of knee osteoarthritis assessment based on gait," *Arch. Comput. Methods Eng.*, vol. 28, no. 2, pp. 345–385, Mar. 2021.
- [14] M. Saleem, M. S. Farid, S. Saleem, and M. H. Khan, "X-ray image analysis for automated knee osteoarthritis detection," *Signal, Image Video Process.*, vol. 14, no. 6, pp. 1079–1087, Sep. 2020.
- [15] J. Abedin, J. Antony, K. McGuinness, K. Moran, N. E. O'Connor, D. Rebholz-Schuhmann, and J. Newell, "Predicting knee osteoarthritis severity: Comparative modeling based on patient's data and plain X-ray images," *Sci. Rep.*, vol. 9, no. 1, pp. 1–11, Apr. 2019.
- [16] J. Antony, K. McGuinness, K. Moran, and N. E. O'Connor, "Automatic detection of knee joints and quantification of knee osteoarthritis severity using convolutional neural networks," in *Proc. 13th Int. Conf. Mach. Learn. Data Mining Pattern Recognit. (MLDM)*. New York, NY, USA: Springer, Jul. 2017, pp. 376–390.
- [17] J. Antony, K. McGuinness, N. E. O'Connor, and K. Moran, "Quantifying radiographic knee osteoarthritis severity using deep convolutional neural networks," in *Proc. 23rd Int. Conf. Pattern Recognit. (ICPR)*, Dec. 2016, pp. 1195–1200.
- [18] F. R. Mansour, "Deep-learning-based automatic computer-aided diagnosis system for diabetic retinopathy," *Biomed. Eng. Lett.*, vol. 8, no. 1, pp. 41–57, Feb. 2018.
- [19] R. Mahum, S. U. Rehman, T. Meraj, H. T. Rauf, A. Irtaza, A. M. El-Sherbeeney, and M. A. El-Meligy, "A novel hybrid approach based on deep CNN features to detect knee osteoarthritis," *Sensors*, vol. 21, no. 18, p. 6189, Sep. 2021.
- [20] C. Cernazanu-Glavan and S. Holban, "Segmentation of bone structure in X-ray images using convolutional neural network," *Adv. Elect. Comput. Eng.*, vol. 13, no. 1, pp. 87–94, 2013, doi: 10.4316/AECE.2013.01015.

- [21] M. Cabezas, A. Oliver, X. Lladó, J. Freixenet, and M. B. Cuadra, "A review of atlas-based segmentation for magnetic resonance brain images," *Comput. Methods Programs Biomed.*, vol. 104, no. 3, pp. e158–e177, Dec. 2011.
- [22] C. Stoloiescu-Crişan and Ş. Holban, "A comparison of X-ray image segmentation techniques," *Adv. Electr. Comput. Eng.*, vol. 13, no. 3, pp. 85–92, 2013.
- [23] H. S. Gan and K. A. Sayuti, "Comparison of improved semi-automated segmentation technique with manual segmentation: Data from the osteoarthritis initiative," *Amer. J. Appl. Sci.*, vol. 13, no. 11, pp. 1068–1075, 2016, doi: 10.3844/ajassp.2016.1068.1075.
- [24] Y. Li, N. Xu, and Q. Lyu, "Construction of a knee osteoarthritis diagnostic system based on X-ray image processing," *Cluster Comput.*, vol. 22, no. S6, pp. 15533–15540, Nov. 2019.
- [25] S. Kubkaddi and K. Ravikumar, "Early detection of knee osteoarthritis using SVM classifier," *Int. J. Sci. Eng. Adv. Technol.*, vol. 5, no. 3, pp. 259–262, 2017.
- [26] Z. Zhu, X. He, G. Qi, Y. Li, B. Cong, and Y. Liu, "Brain tumor segmentation based on the fusion of deep semantics and edge information in multimodal MRI," *Inf. Fusion*, vol. 91, pp. 376–387, Mar. 2023.
- [27] A. Adegun and S. Viriri, "Deep learning techniques for skin lesion analysis and melanoma cancer detection: A survey of state-of-the-art," *Artif. Intell. Rev.*, vol. 54, no. 2 pp. 811–841, Jun. 2020.
- [28] M. A. Guillén, A. Llanes, B. Imbernón, R. Martínez-España, A. Bueno-Crespo, J.-C. Cano, and J. M. Cecilia, "Performance evaluation of edge-computing platforms for the prediction of low temperatures in agriculture using deep learning," *J. Supercomput.*, vol. 77, no. 1, pp. 818–840, Jan. 2021.
- [29] B. Janakiramaiah, G. Kalyani, and A. Jayalakshmi, "Retraction note: Automatic alert generation in a surveillance systems for smart city environment using deep learning algorithm," *Evol. Intell.*, vol. 14, no. 2, pp. 635–642, Dec. 2022.
- [30] A. F. M. Hani, A. S. Malik, D. Kumar, R. Kamil, R. Razak, and A. Kiflie, "Features and modalities for assessing early knee osteoarthritis," in *Proc. Int. Conf. Electr. Eng. Informat.*, Jul. 2011, pp. 1–6.
- [31] A. E. Nelson, F. Fang, L. Arbeeve, R. J. Cleveland, T. A. Schwartz, L. F. Callahan, J. S. Marron, and R. F. Loeser, "A machine learning approach to knee osteoarthritis phenotyping: Data from the FNIH biomarkers consortium," *Osteoarthritis Cartilage*, vol. 27, no. 7, pp. 994–1001, Jul. 2019.
- [32] A. Aprovitola and L. Gallo, "Knee bone segmentation from MRI: A classification and literature review," *Biocybern. Biomed. Eng.*, vol. 36, no. 2, pp. 437–449, 2016.
- [33] V. Pedroia, S. Majumdar, and T. M. Link, "Segmentation of joint and musculoskeletal tissue in the study of arthritis," *Magn. Reson. Mater. Phys., Biol. Med.*, vol. 29, no. 2, pp. 207–221, Apr. 2016.
- [34] J. Kubicek, M. Penhaker, M. Augustynek, I. Bryjova, and M. Cerny, "Segmentation of knee cartilage: A comprehensive review," *J. Med. Imag. Health Informat.*, vol. 8, no. 3, pp. 401–418, Mar. 2018.
- [35] B. Zhang, Y. Zhang, H. D. Cheng, M. Xian, S. Gai, O. Cheng, and K. Huang, "Computer-aided knee joint magnetic resonance image segmentation—A survey," 2018, arXiv:1802.04894.
- [36] T. Meena and S. Roy, "Bone fracture detection using deep supervised learning from radiological images: A paradigm shift," *Diagnostics*, vol. 12, no. 10, p. 2420, Oct. 2022.
- [37] S. Roy, T. Meena, and S.-J. Lim, "Demystifying supervised learning in healthcare 4.0: A new reality of transforming diagnostic medicine," *Diagnostics*, vol. 12, no. 10, p. 2549, Oct. 2022.
- [38] D. Pal, P. B. Reddy, and S. Roy, "Attention UW-Net: A fully connected model for automatic segmentation and annotation of chest X-ray," *Comput. Biol. Med.*, vol. 150, Nov. 2022, Art. no. 106083.
- [39] H. Lee, H. Hong, and J. Kim, "BCD-NET: A novel method for cartilage segmentation of knee MRI via deep segmentation networks with bonecartilage-complex modeling," in *Proc. IEEE 15th Int. Symp. Biomed. Imag. (ISBI)*, Apr. 2018, pp. 1538–1541.
- [40] F. Liu, Z. Zhou, H. Jang, A. Samsonov, G. Zhao, and R. Kijowski, "Deep convolutional neural network and 3D deformable approach for tissue segmentation in musculoskeletal magnetic resonance imaging," *Magn. Reson. Med.*, vol. 79, no. 4, pp. 2379–2391, 2018.
- [41] Z. Zhou, G. Zhao, R. Kijowski, and F. Liu, "Deep convolutional neural network for segmentation of knee joint anatomy," *Magn. Reson. Med.*, vol. 80, no. 6, pp. 2759–2770, Dec. 2018.
- [42] R. Mahum, H. Munir, Z.-U.-N. Mughal, M. Awais, F. S. Khan, M. Saqlain, S. Mahamad, and I. Tlili, "A novel framework for potato leaf disease detection using an efficient deep learning model," *Hum. Ecol. Risk Assessment*, Int. J., vol. 29, no. 2, pp. 303–326, Feb. 2023.
- [43] S. Sikandar, R. Mahmum, and N. Akbar, "Cricket videos summary generation using a novel convolutional

- neural network,” in Proc. Mohammad Ali Jinnah Univ. Int. Conf. Comput. (MAJICC), Oct. 2022, pp. 1–7.
- [44] J. C.-W. Cheung, A. Y.-C. Tam, L.-C. Chan, P.-K. Chan, and C. Wen, “Superiority of multiple-joint space width over minimum-joint space width approach in the machine learning for radiographic severity and knee osteoarthritis progression,” *Biology*, vol. 10, no. 11, p. 1107, Oct. 2021.
- [45] A. Wahid, J. A. Shah, A. U. Khan, M. Ullah, and M. Z. Ayob, “Multilayered basis pursuit algorithms for classification of MR images of knee ACL tear,” *IEEE Access*, vol. 8, pp. 205424–205435, 2020, doi: 10.1109/ACCESS.2020.3037745.
- [46] Y. Wang, X. Wang, T. Gao, L. Du, and W. Liu, “An automatic knee osteoarthritis diagnosis method based on deep learning: Data from the osteoarthritis initiative,” *J. Healthcare Eng.*, vol. 2021, pp. 1–10, Sep. 2021.
- [47] M. S. Swanson, J. W. Prescott, T. M. Best, K. Powell, R. D. Jackson, F. Haq, and M. N. Gurcan, “Semi-automated segmentation to assess the lateral meniscus in normal and osteoarthritic knees,” *Osteoarthritis Cartilage*, vol. 18, no. 3, pp. 344–353, Mar. 2010.
- [48] H.-S. Gan, K. A. Sayuti, N. H. Harun, and A. H. A. Karim, “Flexible non cartilage seeds for osteoarthritic magnetic resonance image of knee: Data from the osteoarthritis initiative,” in Proc. IEEE EMBS Conf. Biomed. Eng. Sci. (IECBES), Dec. 2016, pp. 748–751.
- [49] S. Kashyap, H. Zhang, K. Rao, and M. Sonka, “Learning-based cost functions for 3-D and 4-D multi-surface multi-object segmentation of knee MRI: Data from the osteoarthritis initiative,” *IEEE Trans. Med. Imag.*, vol. 37, no. 5, pp. 1103–1113, May 2018.
- [50] Q. Liu, Q. Wang, L. Zhang, Y. Gao, and D. Shen, “Multi-atlas context forests for knee MR image segmentation,” in Proc. 6th Int. Workshop Mach. Learn. Med. Imag. (MLMI). Munich, Germany: Springer, Oct. 2015, pp. 186–193.
- [51] S. S. Gornale, P. U. Patravali, A. M. Uppin, and P. S. Hiremath, “Study of segmentation techniques for assessment of osteoarthritis in knee X-ray images,” *Int. J. Image, Graph. Signal Process.*, vol. 11, no. 2, pp. 48–57, Feb. 2019.
- [52] H.-S. Gan, K. A. Sayuti, M. H. Ramlee, Y.-S. Lee, W. M. H. W. Mahmud, and A. H. A. Karim, “Unifying the seeds auto-generation (SAGE) with knee cartilage segmentation framework: Data from the osteoarthritis initiative,” *Int. J. Comput. Assist. Radiol. Surg.*, vol. 14, no. 5, pp. 755–762, May 2019.
- [53] J. H. Cueva, D. Castillo, H. Espinós-Morató, D. Durán, P. Díaz, and V. Lakshminarayanan, “Detection and classification of knee osteoarthritis,” *Diagnostics*, vol. 12, no. 10, p. 2362, Sep. 2022.
- [54] L. Anifah, M. H. Purnomo, T. L. R. Mengko, and I. K. E. Purnama, “Osteoarthritis severity determination using self organizing map based Gabor kernel,” *IOP Conf. Ser., Mater. Sci. Eng.*, vol. 306, Feb. 2018, Art. no. 012071.
- [55] K. Duan, S. Bai, L. Xie, H. Qi, Q. Huang, and Q. Tian, “CenterNet: Keypoint triplets for object detection,” in Proc. IEEE/CVF Int. Conf. Comput. Vis. (ICCV), Oct. 2019, pp. 6569–6578.
- [56] H. Law and J. Deng, “CornerNet: Detecting objects as paired keypoints,” in Proc. Eur. Conf. Comput. Vis. (ECCV), 2018, pp. 734–750.
- [57] G. Huang, Z. Liu, L. Van Der Maaten, and K. Q. Weinberger, “Densely connected convolutional networks,” in Proc. IEEE Conf. Comput. Vis. Pattern Recognit. (CVPR), Jul. 2017, pp. 4700–4708.
- [58] B. Xu, N. Wang, T. Chen, and M. Li, “Empirical evaluation of rectified activations in convolutional network,” 2015, arXiv:1505.00853.
- [59] T.-Y. Lin, P. Goyal, R. Girshick, K. He, and P. Dollar, “Focal loss for dense object detection,” in Proc. IEEE Int. Conf. Comput. Vis. (ICCV), Oct. 2017, pp. 2980–2988.
- [60] Y. Liu, K. Chen, C. Liu, Z. Qin, Z. Luo, and J. Wang, “Structured knowledge distillation for semantic segmentation,” in Proc. IEEE/CVF Conf. Comput. Vis. Pattern Recognit. (CVPR), Jun. 2019, pp. 2604–2613.